J-Researchers

Journal of Civil Engineering Researchers

Journal homepage: www.journals-researchers.com

Prediction of Geopolymer Concrete Compressive and Flexural Strengths from Extended Mix Parameters Using Comparative Machine Learning Models

Hassan Siddique [a], Muhammad Rohan Asif [b], Muhammad Saad Abrar [c], Muhammad Sayyam Asif [d*]

[a] Building, Civil and Environmental Engineering Department, Concordia University, Montreal Canada

[b] Military College of Engineering, National University of Sciences and Technology, Risalpur, Pakistan

[c] Department of Civil Engineering, University of New Brunswick, New Brunswick, Canada

[d] Department of Civil Engineering, Ghulam Ishaq Khan Institute of Engineering Sciences and Technology, Topi, Swabi, Pakistan

ABSTRACT

Ordinary Portland cement has high energy and CO_2 footprint, motivating the use of geopolymer concrete as a lower-carbon structural binder. However, geopolymer mix design still relies on slow trial-and-error that does not achieve target compressive and flexural strengths. Prior studies used machine learning to predict geopolymer strength, but mostly with few input variables, compressive-strength-only targets and limited algorithm comparison. Hence, there is no clear evidence on which model best predicts strengths for extended geopolymer mix designs. For this study, a database of 497 geopolymer mixes with fourteen mix and curing variables was compiled from literature, and four supervised models' artificial neural network (ANN), support vector machine (SVM), Gaussian process regression (GPR) and classification and regression tree (CART) were trained on normalized data with tuned hyper-parameters. Model performance was evaluated using correlation coefficient, root mean square error and mean absolute error for separate compressive and flexural targets. All four models achieved high predictive accuracy on test data, with ANN giving the best compressive-strength performance. For flexural strength, SVM provided the most accurate predictions. Different mechanical responses of geopolymer concrete are best represented by different model structures and that multi-parameter machine-learning frameworks can markedly reduce empirical trial batches. Overall, developed comparative machine-learning framework directly addresses limitations of trial-and-error geopolymer mix design by providing practical tool to predict compressive and flexural strengths from mix parameters and to support performance-based, low-carbon mix design. Future work should expand the database to other mechanical and durability properties and embed tools in decision-support software.

ARTICLE INFO

Received: June 14, 2026
Accepted: June 29 , 2026

Keywords:
Geopolymer concrete
Machine learning
Compressive strength
Flexural strength
Sustainable construction

DOI: 10.66224/JCER.8.3.39
DOR: 20.1001.1.22516530.1399.11.4.1.1

* Corresponding author. sayyam.asif@giki.edu.pk

1. Introduction

The most popular artificial binding material is conventional Portland cement because of its qualities such as being affordable, dependable, and easily accessible (Rashiddadash et al., 2014). As the need for construction keeps increasing, it is becoming more well-known (de Brito & Kurda, 2021). The cement business is strongly related to the growth of a country's infrastructure, economy, and the improvement of people's quality of life. The two biggest cement manufacturers, China and India, produced 2.4 billion tonnes and 290 million tonnes of cement, respectively, in 2018 ("Mineral Commodity Summaries 2019," 2019). Demand increased by 12% in 2019, and as urbanization and population growth persist, it is predicted to double by 2050 (N.d., 2022). However, the main problems are the finite natural resources used in production, the lengthy production process, and the high carbon emissions. It consumes a tremendous amount of energy, which is another significant problem. To produce one ton of cement, over 4 GJ of energy is needed, and almost one ton of carbon dioxide is released into the atmosphere (Sivasundaram & Malhotra, 1988). A warning sign for us is the fact that the manufacture of cement accounts for about 5% of global carbon dioxide emissions and 14% of global energy usage (Duxson et al., 2006). To meet the escalating demand, the cement industry must overcome numerous challenges under economic and environmental constraints (Gunasekara et al., 2020). In response to these environmental and energy concerns, alternative binders such as geopolymer concrete have been developed, which utilizes industrial by-products to reduce emissions and resource depletion.

The concept of geopolymer concrete (GPC) was pioneered by Joseph Davidovits in the late 1970s, who proposed the use of inorganic aluminosilicate materials activated by alkaline solutions as a substitute for ordinary Portland cement (OPC). The central idea behind geopolymers is the alkali activation of aluminosilicate precursors such as fly ash, ground granulated blast furnace slag (GGBS), rice husk ash (RHA), and metakaolin to produce a binder with cement-like properties (Davidovits, 1994). In the geopolymerization process, silicon (Si) and aluminum (Al) oxides react with alkali activators like sodium hydroxide (NaOH) and sodium silicate (Na_2SiO_3) under controlled curing conditions to form a rigid three-dimensional aluminosilicate network (Waqas, Butt, Danish, et al., 2021). The resulting product exhibits exceptional compressive and flexural strength, low permeability, and high resistance to chemical attack, positioning it as a sustainable alternative to conventional cementitious systems (Liu et al., 2023). The precursor materials—particularly fly ash and GGBS—are industrial by-products with rich aluminosilicate content. Fly ash contributes to the formation of NASH (sodium aluminosilicate hydrate) gels, while GGBS introduces calcium, which forms CASH (calcium aluminosilicate hydrate) gels that enhance early strength development (Ahmad et al., 2021). The synergy between these materials allows tailoring of mechanical and durability properties by adjusting proportions of the precursor and the activator.

One of the most significant advantages of GPC is its potential to reduce CO_2 emissions. The production of OPC is responsible for approximately 7–8% of global CO_2 emissions, mainly due to the calcination of limestone and the high-temperature processing involved (P. Zhang et al., 2023). In contrast, the production of geopolymer binders can reduce CO_2 emissions by 80–90% depending on the source material and activator used (Oti et al., 2024). Life-cycle assessment (LCA) studies have confirmed the superior environmental performance of GPC. The utilization of industrial by-products such as fly ash, GGBS, and RHA minimizes waste disposal and reduces the demand for virgin raw materials (Waqas, Butt, Danish, et al., 2021). Garcés and colleagues demonstrated that the embodied energy of GPC is five to six times lower than OPC, particularly when waste-derived sodium silicate is used (Garces et al., 2021). Furthermore, the enhanced durability of GPC reduces the maintenance frequency and extends structural lifespan, indirectly contributing to lower environmental impact over time. The absence of calcination and lower curing temperatures further reduce the carbon footprint (P. Zhang et al., 2023). Moreover, geopolymer concretes generally exhibit superior mechanical performance compared to OPC concretes, especially in compressive and flexural strength. Studies by (Liu et al., 2023) and (Ahmad et al., 2021) showed compressive strengths ranging from 60–90 MPa after 28 days, outperforming conventional OPC systems of equivalent grade. Flexural and tensile strengths in GPC also show improvement, attributed to the dense matrix and refined microstructure formed by the coexistence of N–A–S–H and C–A–S–H gels (Ma et al., 2018). The elastic modulus of GPC tends to be comparable to or slightly lower than OPC, depending on the precursor and curing regime (Venkatesh et al., 2024). Similar studies indicate that GPC is a leading candidate for sustainable construction (Figure 1). A. M. Mustafa Al Bakri investigated geopolymer concrete and discovered through experimentation that, when OPC was given better circumstances, geopolymer concrete still obtained over 60% higher strength than OPC (Mustafa et al., 2019). According to Pradip Nath's research, geopolymer concrete outperformed OPC concrete in terms of flexural strength and had around 20%–30% lower elastic modulus than OPC concrete with the same strength (Nath & Sarker, 2017). In addition to this (Garces et al., 2021) Garcés carried out a life-cycle assessment that showed a minimized effect on global warming and aquatic plant growth as compared to OPC.

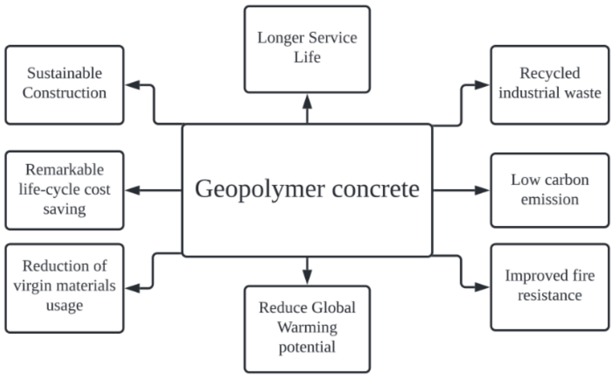

Figure 1. Benefits of using GPC over OPC

The compressive and flexural strength of GPC is influenced by multiple interrelated factors including the type and proportion of binder, activator concentration, and aggregate properties. Fly ash, GGBS, silica fume, and rice husk ash serve as major aluminosilicate sources. The inclusion of GGBS improves early strength due to its calcium content, while silica fume enhances matrix densification (Ahmad et al., 2021). The molarity of NaOH and the ratio of sodium silicate to sodium hydroxide (Na_2SiO_3 /NaOH) significantly affect the polymerization process (Ahmad et al., 2021). The activator modulus (SiO_2 /Na_2O) and water content influence workability and strength development. Higher water content increases workability but decreases compressive strength due to pore formation (Oti et al., 2024). Superplasticizers help achieve required flowability without excess water, while fine and coarse aggregates determine density and modulus (Venkatesh et al., 2024). Curing conditions have a profound influence on GPC's mechanical properties. Heat curing accelerates geopolymerization, yielding higher early-age strength, while ambient curing is slower but advantageous for on-site applications (Pham et al., 2020). Studies have shown that curing at 60–90 °C for 24 hours produces compressive strengths exceeding 70 MPa for fly ash–GGBS blends (Ahmed et al., 2021).

However, extended curing times or excessive temperature may cause microcracking due to rapid water evaporation (Waqas, Butt, Danish, et al., 2021). The choice between ambient and heat curing depends on precursor reactivity and application environment. Recent work has demonstrated that with optimized activator ratios and GGBS content, ambient-cured GPC can achieve strengths comparable to heat-cured systems (H. Zhang et al., 2020).

Despite a lot of research on geopolymer concrete, mix-design procedure is still uncertain. Attaining specific mechanical properties of geopolymer concrete requires a suitable mix design. Many researchers attempted to develop a mix design, but most of their work was based on a trial-and-error approach, which is very time- and resource-consuming (Albitar et al., 2017; Anuradha et al., 2013; Ferdous et al., 2015; Ma et al., 2018; Naghizadeh & Ekolu, 2019; Panda & Tan, 2018; Somna et al., 2011). Given the number of interacting parameters, binder composition, activator modulus, curing regime, and admixtures, GPC mix design remains largely empirical (Montes & Allouche, 2013). Traditional trial-and-error methods are time-consuming, material-intensive, and lack predictive precision (Rehman & Khokhar, 2022). Empirical correlations often fail to capture nonlinear relationships between inputs and strength outcomes. Consequently, researchers have increasingly turned to data-driven and machine learning approaches for mix optimization.

Machine learning (ML) has emerged as a transformative tool in civil materials engineering, enabling accurate prediction of concrete mechanical properties from input parameters. Studies like (Ben Chaabene et al., 2020) and subsequent works established that algorithms such as artificial neural networks (ANN), support vector machines (SVM), Gaussian process regression (GPR), decision trees (DT), and adaptive neuro-fuzzy inference systems (ANFIS) are effective for predicting compressive strength. Common inputs include mix proportions and curing conditions, while compressive strength remains the most frequent output. (Van Dao et al., 2019) employed ANFIS and ANN to predict compressive strength of fly ash-based GPC using inputs such as NaOH molarity, Na_2SiO_3 content, and curing time. Their ANN model achieved R^2 values above 0.9, demonstrating strong predictive capacity but limited input scope. Similarly, Topcu (2008)developed literature-based datasets for GPC and employed fuzzy logic and ANN for compressive strength prediction. Despite high correlation, the models lacked consideration of curing temperature and superplasticizer effects.

Recent advances include ensemble and deep learning models. (Ahmad et al., 2021) compared ANN, AdaBoost, and boosting techniques, finding ensemble methods (R^2 = 0.96) more accurate than standalone ANN. Amin (2022) used 156 datasets and found that random forest and bagging ensemble models yielded superior prediction performance compared to SVM and DT. Yılmaz (2024) employed XGBoost for both compressive and flexural strength prediction, achieving R^2 = 0.98 for compressive and 0.90 for flexural strength, indicating the promise of ensemble ML in modeling nonlinear relationships. By capturing nonlinear relationships among variables, machine learning techniques help transition from empirical mix design toward predictive, performance-driven formulations. Nevertheless, in most existing studies the input features are limited to 4–8 variables, omitting critical factors such as activator modulus, curing regime, aggregates, and superplasticizers (Rehman & Khokhar, 2022) and few studies systematically compare multiple algorithms using the same GPC dataset (Amin et al., 2022). This study therefore, aims, to develop machine learning models that predict the compressive and flexural strengths of geopolymer concrete using an extended set of mix and curing parameters and to compare the predictive performance of these machine learning models and identify the most accurate model for supporting sustainable geopolymer concrete mix design.

2. Materials and Methods

The methodological framework was designed to move from empirical, trial-and-error mix design toward a predictive, data-driven approach for geopolymer concrete. Most existing machine learning models for GPC compressive strength rely on fewer input variables. The methodology begins with the construction of a consolidated experimental database of geopolymer mixes, in which fourteen mix and curing parameters are assembled from published studies together with 28-day compressive and flexural strengths. These variables capture binder composition, activator chemistry, water and admixture contents, aggregate skeleton and curing conditions, reflecting the key strength-controlling factors highlighted in previous work.

The compiled dataset is then preprocessed through outlier screening and normalization, and partitioned into training and testing subsets. Obvious data entry errors and physically implausible values (e.g. negative strengths, unrealistically high binder contents) were removed by visual inspection; remaining points were retained to preserve the full variability of published mixes. On this common dataset, four supervised machine learning families are trained separately for compressive and flexural strength prediction. Model performance is quantified using correlation coefficient, root mean square error and mean absolute error, enabling a systematic comparison across algorithms (Figure 2).

2.1. Data Collection

Several input parameters are required by machine-learning algorithms to deliver precise results. A total of 497 data points were gathered from previous publications, including 16 instances compiled from multiple studies (Abdelmonim & Bompa, 2021; Ahmed et al., 2021; Asayesh et al., 2021; Chen et al., 2021; Deb et al., 2014; Ding et al., 2018; Esparham & Mohammadi, 2022; Fang et al., 2018; Faridmehr et al., 2021; Gunasekara et al., 2020; Gupta et al., 2021; Hadi et al., 2017; John et al., 2021; Kanagaraj et al., 2022; Kishore et al., 2022; B. S. C. Kumar, 2019; Lee t al., 2020; Lopes et al., 2020; Malayali et al., 2021; Mohammed Hameed & Mohammed Ali, 2021; Nath & Sarker, 2015, 2017; Padakanti et al., 2022; Pan et al., 2011; Patel & Shah, 2018; Pham et al., 2020; Rahman & Al-Ameri, 2021; Rahmawati et al., 2021; Reddy et al., 2018; Simatupang et al., 2019; Sitarz et al., 2020, 2021; Sravanthi et al., 2020; Subash et al., 2021; Verma et al., 2022; Q. Wang et al., 2022; W.-C. Wang et al., 2015; Waqas, Butt, Danish, et al., 2021; Waqas, Butt, Zhu, et al., 2021; Zaidahtulakmal et al., 2019; H. Zhang et al., 2020; Zhao et al., 2021).

The dataset included Fly Ash, Silica Fume, Ground Granulated Blast Furnace Slag (GGBS), Rice Husk Ash (RHA), NaOH, NaOH molarity, Na_2SiO_3, SiO_2/Na_2O ratio, water, superplasticizer, heat-curing [ambient-curing] time and temperature, coarse aggregate, and fine aggregate as input parameters, with two output variables, compressive strength and flexural strength.

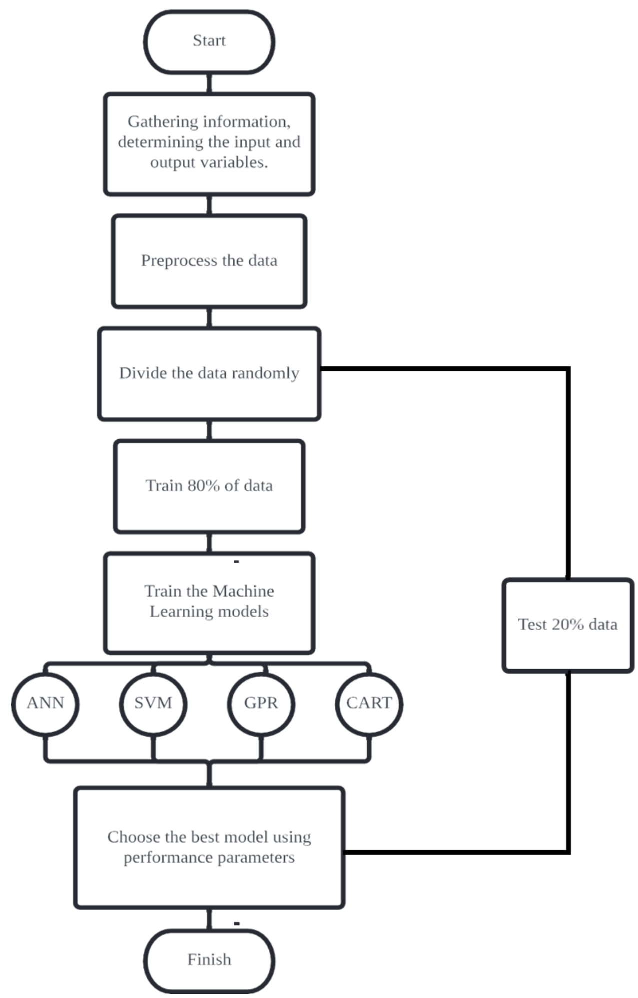

Figure 2. The proposed machine-learning workflow used in this study.

Figure 3 illustrates the distribution of the fourteen input parameters used to develop the machine-learning models and highlights how the compiled database spans a wide but realistic range of geopolymer concrete mix designs. Coarse aggregate content shows a distinctly bimodal pattern, with one cluster of mixes containing little or no coarse aggregate, representing mortar-type or paste-rich geopolymer systems—and a second group centred around conventional concrete aggregate contents of roughly 1200–1500 kg/m³. This confirms that the dataset captures both highly aggregate-rich structural concretes and mixes designed primarily to study binder effects. Fine aggregate content, in contrast, follows a broad but largely unimodal distribution concentrated between about 600 and 1000 kg/m³, indicating that sand proportions are generally kept within traditional concrete ranges so that variability in strength is driven more by binder chemistry, activator composition, and curing than by extreme changes in fine aggregate volume.

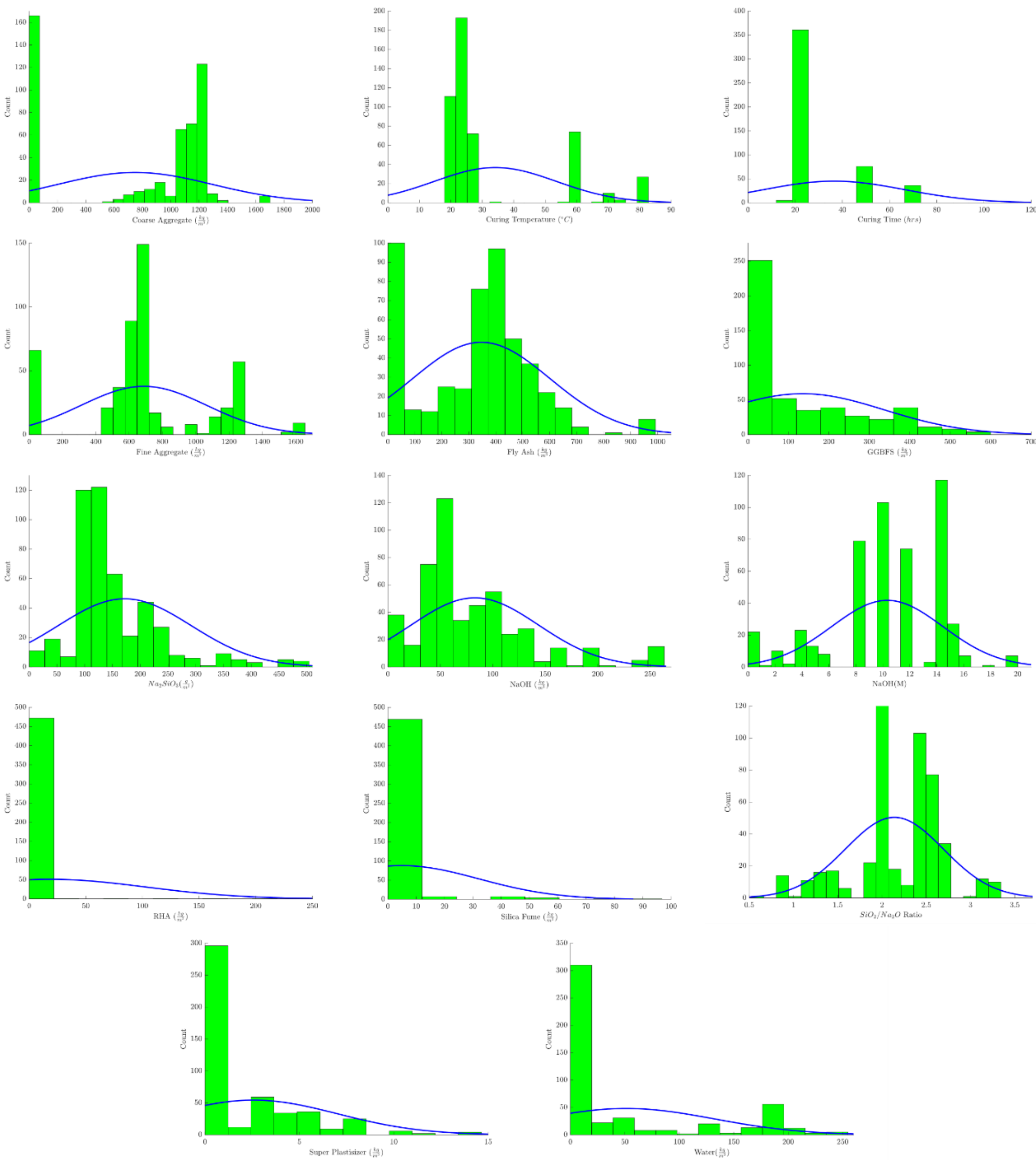

Figure 3. Histogram distributions of the fourteen input parameters

The binder histograms emphasize the dominance of fly ash–based systems. Fly ash content is heavily represented between approximately 300 and 600 kg/m³, with a taper towards very high dosages, showing that most mixtures rely on fly ash as the primary aluminosilicate precursor. Ground-granulated blast furnace slag (GGBS) exhibits a right-skewed distribution, with many mixes using modest slag contents around 100–300 kg/m³ and relatively few very high-slag formulations. This reflects the common practice of incorporating slag as a partial replacement to boost early-age strength and modify gel chemistry rather than as the sole binder. Rice husk ash (RHA) and silica fume appear in only a small fraction of the data; their histograms are dominated by zero values with a limited number of non-zero entries. This pattern indicates that these finely divided pozzolanic materials are used as supplementary components to refine the microstructure or enhance specific durability aspects in selected studies, while the bulk of mixes are formulated without them.

The activator-related variables also reveal important trends. Sodium hydroxide (NaOH) content is concentrated in a relatively narrow band, generally between about 100 and 200 kg/m³, indicating that most researchers work within a constrained dosage window that is known to provide sufficient alkalinity for geopolymerization without causing excessive efflorescence or handling issues. NaOH molarity displays an even tighter clustering, with most data points between 8 and 14 M; this aligns with the commonly recommended concentration range where dissolution of the aluminosilicate precursors and subsequent gel formation are most efficient. Sodium silicate (Na_2SiO_3) content shows a right-skewed distribution with many mixes at moderate dosages and progressively fewer at high values, suggesting that the silicate component is varied within practical limits to adjust the Si/Al ratio and viscosity of the activator solution. The SiO_2/Na_2O ratio, which represents the activator modulus, is concentrated mainly between about 1.5 and 2.8. This compact distribution around the optimum window reported in the literature confirms that the compiled database is centred on chemically efficient activator formulations rather than experimental extremes, ensuring that the machines learn from mixes that are both realistic and well-performing.

Workability-controlling parameters show similarly characteristic behavior. Water content declines steeply from low to high values, with most mixes lying in the lower range that corresponds to the low water-to-binder ratios typical of high-performance geopolymer systems. This dominance of low-water mixtures indicates that the dataset is biased towards dense, high-strength concretes rather than very fluid, low-strength mortars, which is appropriate for a study focused on mechanical performance. Superplasticizer dosage is heavily right-skewed, most mixtures contain zero or very small quantities of superplasticizer, while only a few employs higher dosages. This suggests that most formulations rely primarily on adjustments in water content and activator proportions to achieve workable mixes, using chemical admixtures only in selected cases such as self-compacting or highly flowable GPC.

The curing-related histograms underline the mixture of laboratory and field-oriented conditions represented in the database. Curing temperature distribution reveals two dominant regimes, a large cluster at ambient temperatures around 20–30 °C and a smaller but distinct population at elevated temperatures between about 60 and 90 °C. This reflects the combination of ambient-cured mixes, which are more representative of in-situ applications, and heat-cured mixes used in many experimental programmes to accelerate geopolymerization and study early-age behavior. Curing time is strongly right-skewed, with a pronounced peak at 24 hours and relatively few data points at longer durations, confirming that one-day heat curing is the de facto standard in most studies. Longer curing periods appear less frequently, indicating that their influence on model training will be modest and predictions for very long heat-curing regimes should be interpreted with some caution.

The compiled dataset spans a rich and diverse but still realistic design space, it includes paste-rich and aggregate-rich concretes, fly-ash-dominant and slag-modified binders, mixes with and without supplementary materials such as RHA and silica fume, a wide range of activator dosages and moduli within practically optimal windows, and both ambient- and heat-curing conditions. This diversity is crucial for training robust machine-learning models capable of capturing the complex, nonlinear relationships between mix design parameters and both compressive and flexural strengths, while the presence of clear peaks and clusters ensures that the models are grounded in the parameter ranges most encountered in practice.

2.2. Hyper-Parameter Tuning

One of the most important stages in machine learning is hyper-parameter tuning, which helps determine the optimal parameters of a model to produce the most precise results. For every algorithm, the key control parameters were adjusted separately for compressive strength and flexural strength until a good balance between accuracy and generalization was achieved. For the ANN, the parameter that needs to be tuned is the number of neurons, and similar adjustments are required for the other models' parameters.

To determine the optimal parameters that prevent overfitting and underfitting while improving the model's accuracy, a trial-and-error method was used. The ideal parameters for the different machine-learning models are shown in Table 1 below.

Table 1.
Tuned hyperparameters of the GPR, SVM, CART and ANN models used to predict compressive and flexural strengths of geopolymer concrete.

Model / Hyper-Parameter	Compressive Strength	Flexural Strength
GPR		
Sigma	88.567	0.0002
Basis Function	zero	zero
Kernel Function	Isotropic Matern 3/2	Non-isotropic Squared
Kernel Scale	192.1645	Auto
Standardize	TRUE	TRUE
SVM		
Box Constraint	126.4457	0.0299
Kernel Scale	78.7904	–
Epsilon	0.1159	0.0443
Kernel Function	Gaussian	Cubic
Standardize	FALSE	TRUE
CART		
Maximum Depth	12	13
Minimum Leaf Size	2	3
ANN		
Neurons per Hidden Layers	12	7-8

2.3. Normalization

The ranges of the data obtained from earlier literature were in raw form and frequently varied, which may affect the model's performance. Therefore, normalizing the data to a range from 0 to 1 was required to reduce the model's bias toward parameters with larger magnitudes. The data were normalized using the formula shown below:

$$v^* = \frac{v - v_{\min}}{(v_{\max} - v_{\min})}$$

where v is the value of any parameter, and v_minand v_maxare the minimum and maximum values of that parameter. The equation gives v^*, which is the normalized value of v. For each input variable, the parameters v_min and v_max were computed from the training data only, and the same scaling factors were then applied to transform the held-out testing samples, so that no information from the test set leaked into the normalization step.

2.4. Machine learning Models

The word "ANN" refers to a computational model that was inspired by biological processes and operates similarly to human neurons. Three fundamental factors make up this model: an input layer, an output layer, and a hidden layer. However, there are some other factors as well, but these three factors are considered standard. The layers are interconnected to enable data transfer and learning. In this study, the input and output parameters were fixed. The hidden layer is a data-dependent parameter that specifies the model's complexity. The model may match the data better if there are more hidden layers present, but this can lead to a problem known as overfitting. Overfitting occurs when the model fits the training dataset perfectly but performs poorly on unseen testing data (Khokhar et al., 2021). Only neurons in the hidden layers exchange information. They are the components of the internal pattern that defines the problem's solution. Most functions, according to theory, can be approximated by a single hidden layer (Agatonovic-Kustrin & Beresford, 2000). Therefore, in this study, the ANN model was trained using multiple hidden layers, and the most appropriate number of layers was selected by comparing the RMSE values for training and validation datasets. The typical structure of the ANN model is shown in Figure 4

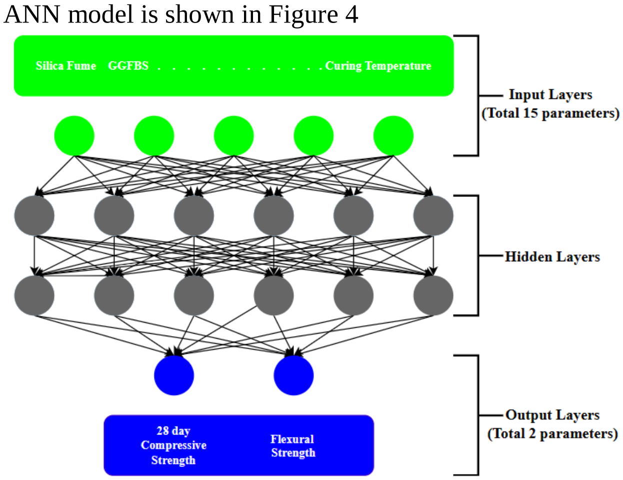

Figure 4. ANN Model framework used for this study

A popular supervised learning method is the Support Vector Machine (SVM) algorithm, which is based on principles of statistics. Support vectors can be used for both classification and regression. An algorithm for maximizing a specific mathematical function with respect to a given dataset is known as SVM. The essence of SVM can be understood by assimilating the concepts of the maximum-margin function, separating hyperplane, soft margin, and kernel function. The maximum-margin hyperplane treats the objects that are to be classified in a multidimensional space as points and then finds a line (or hyperplane) that separates the points (Figure 5). The separating hyperplane is considered a fundamental part of the success of SVM. SVM does not assume any specific probability distribution or functional form for the data; it only assumes that the training and testing samples are drawn from the same underlying distribution.

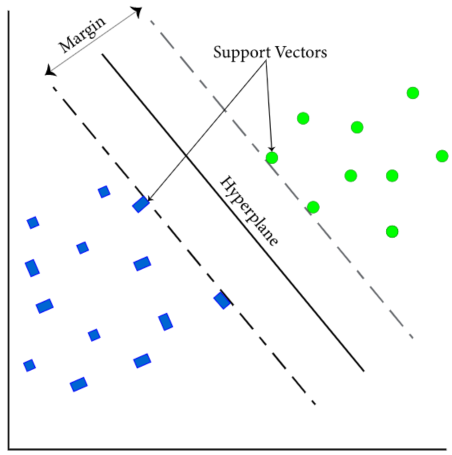

Figure 5. Schematic diagram of the support vector machine (SVM).

The soft margin allows certain points in the dataset to pass through the separating hyperplane's margin without significantly affecting the outcome (Noble, 2006). The kernel function is used in SVM when there is a need for nonlinear modeling in higher dimensions because the SVM algorithm was originally proposed for constructing a linear model. A kernel function in nonlinear modeling can add extra dimensions to the actual data and transform it into a linear model in the resultant higher-dimensional space, as shown in Figure 5. Mathematically, it can be expressed as:

$$f(x, y) = g(x) \cdot g(y)$$

where f is the kernel function, x and y are input parameters in an n-dimensional space. The function f converts the input from n to m dimensions using the dot product of g(x) and g(y) (Topçu & Sarıdemir, 2008).

The Bayesian probability theory-based technique known as Gaussian Process Regression (GPR) has been successful in estimating points in dispersed data.

It is a nonlinear, probabilistic, and non-parametric method that is utilized across a variety of domains to identify patterns in complex datasets (Cheng et al., 2014; Omran et al., 2016).

GPR is represented by the equation:

$$D = \{(a_i, b_i)\}, i = 1,2, \dots, N$$

where a_i is the input factor and b_i is the corresponding target factor. As a Gaussian process of its mean function and covariance function, Gaussian Process Regression can be defined as (Banerjee et al., 2008):

$$f(a) = GP[m(a), k(a, a')]$$

where k(a, a′) describes the use of data at one location to forecast data at another. The mean function, denoted by m(a), describes the complete set of data by identifying its centre.

The following equation represents the relationship between the input and output variables:

$$y = f(a)$$

However, there is usually some data noise in real-world problems; therefore, an epsilon (ε) factor must be considered. Consequently, the relationship becomes:

$$y = f(a) + \varepsilon$$

Classification and Regression Tree (CART) divides the input data into two mutually exclusive groups using a heuristic technique. It is an inverted tree structure consisting of nodes. CART can be trained for either classification or regression, depending on the type of input data. It starts with the initial root node, which is then divided into two sub-nodes, each representing a separate category. After further dividing these sub-nodes, the process is repeated until the leaf nodes are reached. A variable is chosen at each node to partition the data. Figure 7 shows the typical CART model. Depending on the dataset, different impurity metrics can be used to determine data splits; however, the Gini index is most used to measure the impurity of sub-nodes that contain the data subsets (Put et al., 2003).

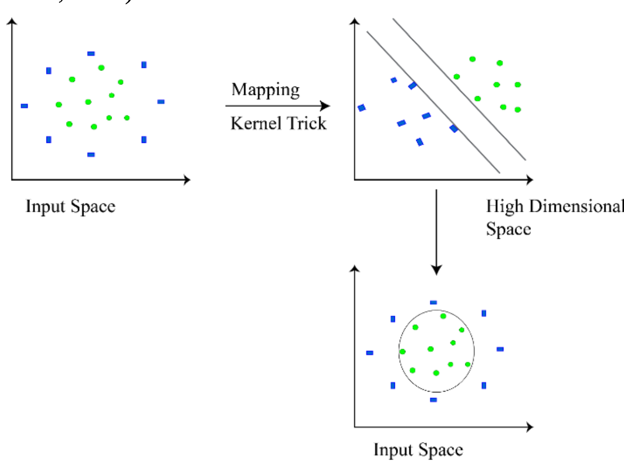

Figure 6. Representation of the kernel function used for nonlinear mapping in SVM.

2.5. Training

The machine-learning models were trained using all hyper-parameters listed in Table 1. Special consideration was given to ensuring that the models were neither under-fitted nor over-fitted. After the training phase was complete, the performance of each model for both the training and testing sets was calculated individually using the performance parameters defined in this section. Figure 2 depicts the method used to train the model.

2.6. Performance Parameters

The performance of the models was assessed using three commonly used performance parameters namely Correlation coefficient (R), Root Mean Square Error (RMSE), Mean Absolute Error (MAE). The parameters are defined using the equations below:

$$R = \frac{\sum_{i=1}^{N}(a_i - \bar{a})(a_i' - \bar{a}')}{\sqrt{\sum_{i=1}^{N}(a_i - \bar{a})^2 \sum_{i=1}^{N}(a_i' - \bar{a}')^2}}$$

$$RMSE = \sqrt{\frac{1}{N}\sum_{i=1}^{N}(a_i' - a_i)^2}$$

$$MAE = \frac{1}{N}\sum_{i=1}^{N} | a_i - a_i' |$$

where a' is the predicted value, a is the actual value $\bar{a}$and $\bar{a}'$are the mean actual and mean predicted values, respectively, and N is the number of data samples. R is optimal when it approaches 1, but values exceeding 0.80 indicate a significant relationship. RMSE is the most frequently employed loss function, while MAE measures the absolute deviation between predicted and actual values. Lower RMSE and MAE values indicate better model performance, as they represent smaller prediction errors.

2.7. Experimental validation mixes

To provide an independent check on the predictive capability of the trained machine-learning models, an additional set of geopolymer concrete mixes was prepared and tested in the laboratory. Three mix designs, denoted as Mix A, Mix B and Mix C, were proportioned within the bounds of the compiled database to represent typical structural geopolymer concretes with varying binder composition and activator content. Each mix employed a binary fly ash–GGBS binder system with total binder content in the range usually adopted for high-performance geopolymer concrete, natural river sand as fine aggregate, and crushed coarse aggregate with a maximum size of 19 mm. The sodium hydroxide solution and sodium silicate solution were dosed to achieve target molarity and SiO_2 /Na_2 O ratios consistent with the central range of the training data.

Standard cylindrical and prismatic specimens were cast from each mix to determine 28-day compressive and flexural strengths. For compressive strength, concrete cylinders with a diameter of 100 mm and height of 200 mm were cast, compacted in two layers on a vibrating table, demoulded after 24 hours and then cured at ambient laboratory conditions until testing. Compressive strength tests were carried out at 28 days in a servo-controlled compression testing machine in accordance with ASTM C39/C39M (or equivalent EN 12390-3), using a controlled loading rate and recording the maximum load at failure.Flexural strength was determined on prismatic beams with nominal dimensions of 100 × 100 × 500 mm, prepared from the same batches as the compressive specimens.

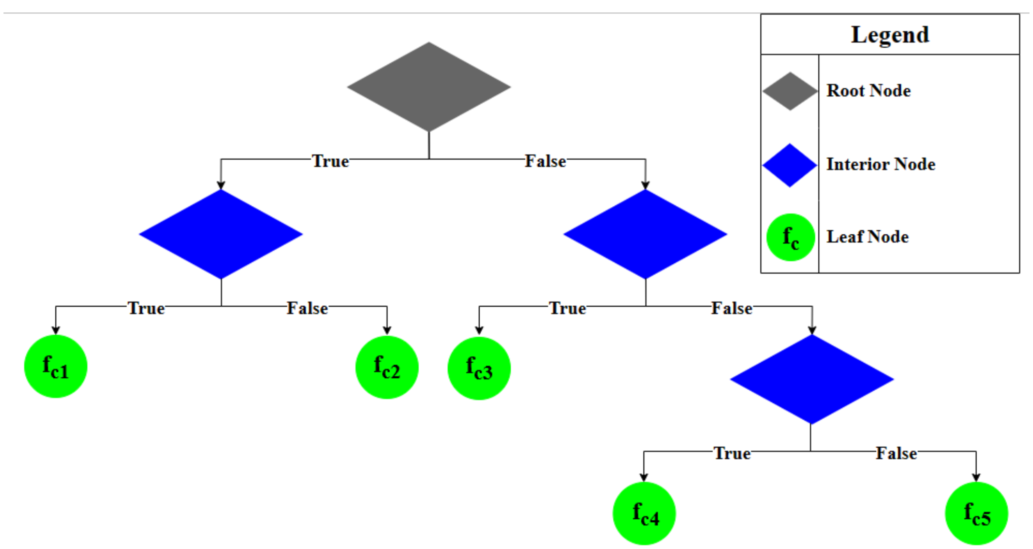

Figure 7. Typical structure of the Classification and Regression Tree (CART) model.

The beams were demoulded after 24 hours and cured under the same conditions as the cylinders. At 28 days, third-point loading tests were performed following ASTM C78/C78M (or equivalent EN 12390-5). The flexural strength (modulus of rupture) was calculated from the maximum load at failure and the specimen geometry. For each mix, at least three replicate specimens were tested in compression and flexure, and the average values were used as the reference "actual" strengths.

The corresponding input parameters for Mix A, Mix B and Mix C (binder components, activator contents and ratios, aggregate contents, water and admixture dosages, and curing regime) were then fed to the best-performing models. The predicted 28-day compressive and flexural strengths were compared directly with the measured values. This experimental verification step provides a practical assessment of the models' generalization capability for previously unseen geopolymer mixtures within the design space covered by the training data.

3. Analysis and Results

The predictive performance of the developed models for estimating compressive and flexural strength was evaluated using key statistical indicators: RMSE and MAE to measure prediction error, and the correlation coefficient (R) to assess how closely the model outputs matched the actual values. A higher R value, closer to 1, indicates a stronger predictive relationship, while lower RMSE and MAE values reflect reduced error and greater accuracy.

For compressive strength, the training RMSE values obtained from the ANN, CART, GPR, and SVM models were 3.90, 4.85, 4.65, and 5.60, respectively, indicating that ANN produced the lowest training error among the four techniques. During testing, the RMSE values increased slightly, with ANN, CART, GPR, and SVM recording 4.50, 5.86, 7.19, and 6.88, respectively. The corresponding RRR values for training compressive strength were 0.9494 (ANN), 0.9202 (CART), 0.9643 (GPR), and 0.9486 (SVM), indicating a high level of agreement between predicted and observed values. In the testing stage, the RRR values remained strong, at 0.9202, 0.9219, 0.8831, and 0.8944 for ANN, CART, GPR, and SVM, respectively. Overall, ANN provided the best balance of low error and high correlation for compressive strength prediction.

A similar trend was observed for flexural strength prediction. The RMSE values for the training datasets were 0.6711, 0.4415, 0.9746, and 0.5078 for ANN, CART, GPR, and SVM, respectively, while for the testing datasets the RMSE values increased slightly to 1.06, 0.6077, 0.7052, and 0.7293. The corresponding RRR values for training were 0.9647 (ANN), 0.9643 (CART), 0.9746 (GPR), and 0.9539 (SVM), demonstrating strong predictive capability for all four models. Testing RRR values were 0.9353, 0.9327, 0.9746, and 0.9000, respectively, with GPR achieving the highest correlation on both training and testing sets, while CART yielded the lowest RMSE values. Taken together, these metrics indicate that GPR is slightly superior for flexural strength prediction, with CART as a close alternative in terms of error magnitude. Figure 8 presents a comparative visualization of these performance parameters, providing a graphical summary of how each modeling technique performed in predicting both compressive and flexural strength.

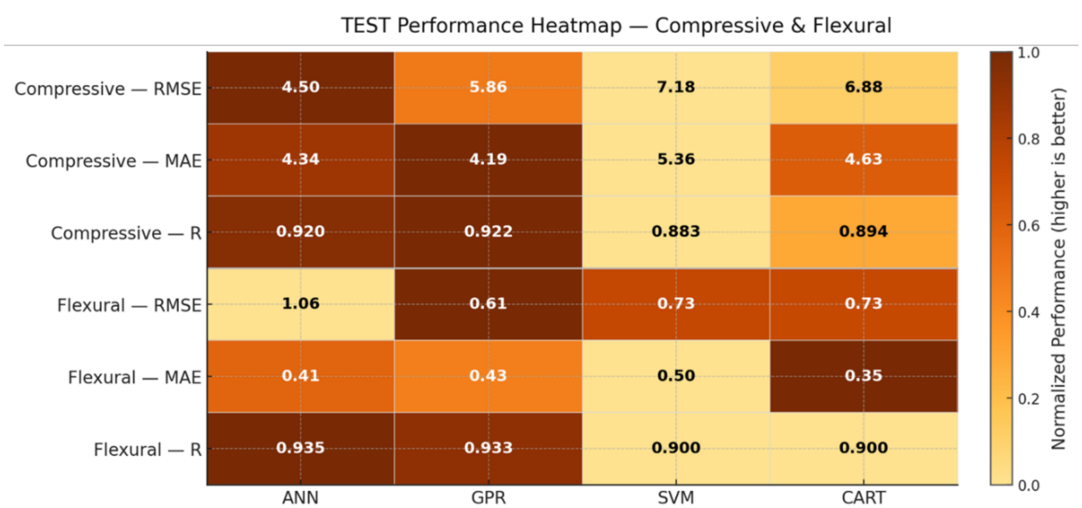

Figure 8. Performance evaluation of all machine-learning models for predicting the compressive and flexural strength of geopolymer concrete using RMSE, R, and MAE for both training and testing datasets.

To further illustrate the predictive capability of each algorithm, scatterplots comparing actual and predicted values for both training and testing datasets were generated for all models. These plots provide a direct visual assessment of how closely the model outputs align with experimental data. In each scatterplot, the black diagonal line represents the ideal fit (Actual = Predicted). Points clustered closely around this line indicate high predictive accuracy.

As observed, ANN and GPR produce tighter clusters for compressive strength, whereas SVM shows better alignment for flexural strength. The CART model exhibits comparatively greater dispersion, particularly in the testing dataset, indicating slightly lower generalization performance.

3.1. Validation of Predictive Models

It is obvious that contrasted with alternative models, the ANN has the highest level of accuracy for compressive strength and SVM for flexural strength. As a result, respective models were utilized to forecast the compressive and flexural strengths of samples that weren't included in any dataset. To validate the model, published experiment results were used in practice.

The input parameters of these samples were provided to the model and the outputs were collected. These output results are compared to the actual results. In addition to validation through published datasets, experimental verification was also performed using geopolymer concrete samples prepared in the laboratory. Three mixes (Mix A, Mix B, and Mix C) were cast and tested for 28-day compressive and flexural strength using standard procedures.

The same input proportions for each mix were then fed into the best-performing models (ANN for compressive strength and SVM for flexural strength) to obtain predicted values.

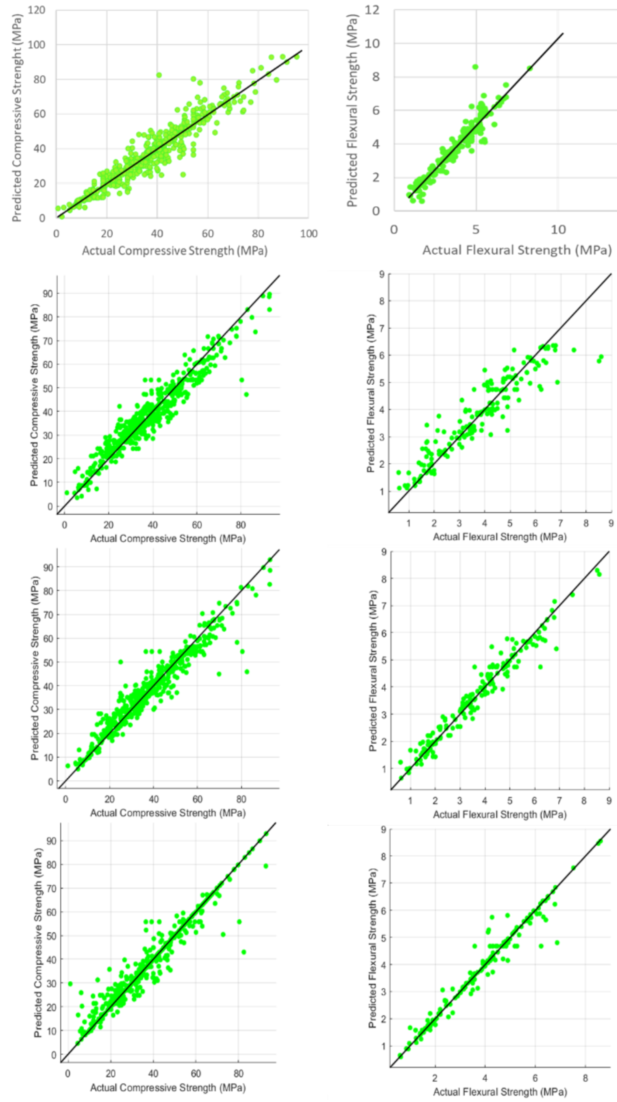

Figure 9. (a–h). Actual vs predicted compressive and flexural strength for all machine-learning models. (a) ANN Training, (b) ANN Testing, (c) CART Training, (d) CART Testing, (e) GPR Training, (f) GPR Testing, (g) SVM Training, (h) SVM Testing)

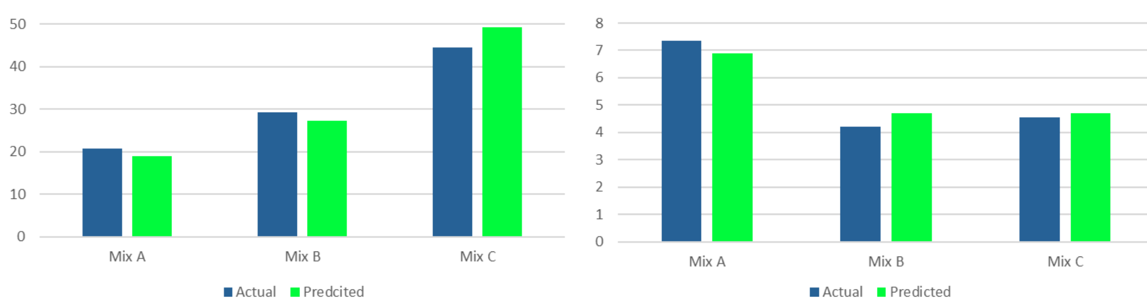

Figure 10. Experimental validation of the predictive models using laboratory-prepared geopolymer concrete samples. (a) Comparison of actual and predicted compressive strength for Mix A, Mix B, and Mix C using the ANN model. (b) Comparison of actual and predicted flexural strength for Mix A, Mix B, and Mix C using the SVM model.

Table 2.
Summary of Comparative Insights

Model	Strength Type	Typical R / R²	RMSE (MPa)	Supporting Studies
ANN	Compressive	0.94–0.99	3–5	(Kurhade S., 2024)
SVM	Flexural	0.95–0.99	0.5–1.0	(Philip et al., 2024)
GPR	Compressive/Flexural	0.95–0.97	2–4	(Haruna H.; Umar, I.; Shao, J.; Adamu, M.; Ibrahim, Y., 2022)
CART	Compressive	0.85–0.90	5–7	(Ren et al., 2021)

The comparison indicates that both models predict the laboratory strengths with reasonable accuracy, showing deviations within acceptable engineering limits. The trends demonstrate that the models capture the combined influence of mix constituents and curing conditions effectively, even for previously unseen compositions. This practical validation confirms the reliability and applicability of the developed models for real-world geopolymer concrete strength estimation.

4. Discussion

The dominance of ANN in compressive strength prediction in this study mirrors findings of (Awoyera et al., 2020) reporting strong correlations ($R^2 > 0.95$) between predicted and actual strengths. The ANN's nonlinear adaptability and capacity to learn hidden patterns in mix proportions, especially NaOH molarity, GGBS, and curing temperature, make it particularly effective. GPR results ($R \approx 0.96$) are consistent with studies where GPR achieved similar or superior accuracy to ANN (Haruna H.; Umar, I.; Shao, J.; Adamu, M.; Ibrahim, Y., 2022; A. Kumar et al., 2022). GPR's probabilistic approach and kernel flexibility make it robust in small-sample environments SVM performed best for flexural strength is reinforced by (Philip et al., 2024), both identifying SVM's superior performance in flexural strength ($R^2 \approx 0.99$). Its margin-based optimization allows precise mapping of multivariate nonlinearities, explaining your high R-values. Conversely, several studies noted its limitations in compressive strength tasks (da Paixão et al., 2022), due to kernel sensitivity. CART's underperformance in this study (RMSE = 5.86 MPa, $R \approx 0.89$) matches prior reports (Ahmad et al., 2022; Ren et al., 2021). CART's simplicity makes it prone to overfitting when not used in ensemble form.

The close agreement between your predicted and experimentally validated strengths (deviation < 5%) supports the reliability of the developed models. The experimental validation phase strengthens robustness compared to others relying solely on computational datasets. Validation through physical testing is essential to prevent model overfitting—a limitation observed in (da Paixão et al., 2022) and (Ahmad et al., 2022), where accuracy dropped on external validation sets.

5. Conclusion and Recommendations

This study developed a data-driven framework to predict the compressive and flexural strengths of geopolymer concrete using machine learning. A consolidated database of 497 mixes with fourteen mix and curing parameters was used to train and test four supervised models: artificial neural network (ANN), support vector machine (SVM), Gaussian process regression (GPR), and classification and regression tree (CART). The input space covered binder composition, activator chemistry, water and superplasticizer contents, aggregates, and curing regime, while the outputs were 28-day compressive and flexural strengths.

All four algorithms were able to capture the nonlinear relationships between geopolymer mix parameters and strength with good accuracy, clearly outperforming simple empirical approaches. For compressive strength, the ANN model achieved the best balance of accuracy and generalization, with high correlation coefficients ($R > 0.92$) and low RMSE and MAE on both training and testing sets. For flexural strength, the SVM model provided the most accurate predictions, again achieving high R values and low error metrics on unseen data. These results show that different mechanical responses of geopolymer concrete may be best represented by different model structures, with ANN particularly suitable for highly nonlinear compressive behavior and SVM better capturing the flexural response.

The best-performing models were further validated using independent literature data and laboratory-cast geopolymer mixes. Predicted strengths were in close agreement with measured values, with deviations remaining within acceptable engineering limits. This confirms that the proposed framework is not only statistically sound but also practically applicable for real-world mixtures within the parameter ranges covered by the database.

From a practical viewpoint, the developed models can be used as predictive tools to support mix design and material selection for geopolymer concrete. By estimating compressive and flexural strengths from input parameters before casting, they can reduce the number of trial batches, save time and material costs, and facilitate the efficient use of industrial by-products such as fly ash, GGBS, RHA, and silica fume. In doing so, they contribute to more sustainable construction practices by lowering experimental effort and supporting the wider adoption of low-carbon binders.

Although the proposed models perform well within the investigated range, several extensions are recommended. First, future work should extend the framework to other key properties of geopolymer concrete, such as modulus of elasticity or splitting tensile strength. Second, hybrid and ensemble learning strategies, such as stacking, boosting, or combinations of ANN, SVM, and tree-based models, could be explored to further reduce prediction errors and provide uncertainty estimates alongside point predictions. Such probabilistic outputs would be valuable for reliability-based design and risk-informed decision-making. Finally, the validated models can be embedded into user-friendly tools or decision-support platforms for designers and practitioners. Linking these tools with optimization routines and with environmental assessment models would help translate the present methodological advances into practical guidelines for sustainable geopolymer concrete production and use.

CRediT authorship contribution statement

Hassan Siddique: Conceptualization, Methodology, Data curation, Writing – original draft.

Muhammad Rohan Asif: Methodology, Formal Analysis, Visualization.

Muhammad Saad Abrar: Support with analysis, Methodology, Writing - original draft.

Muhammad Sayyam Asif: Literature review, Writing - Review and edit, Reference Management.

Declarations

Funding

No funding was received to assist with the preparation of this manuscript.

Competing Interests

The authors have no competing interests to declare that are relevant to the content of this article.

Ethics Approval and Consent to Participate

Ethics and Consent to Participate declarations: not applicable.

Data Availability Statement

The datasets used and/or analysed during the current study are available from the corresponding author upon reasonable request.

Acknowledgement

The authors used Grammarly (Grammarly Inc.) to improve grammar, wording clarity, and caption consistency. No AI tools were used for data collection, analysis, figure generation, or to create scientific content. All machine-assisted edits were reviewed and verified by the authors.

References

[1] Abdelmonim, A., & Bompa, D. V. (2021). Mechanical and Fresh Properties of Multi-Binder Geopolymer Mortars Incorporating Recycled Rubber Particles. Infrastructures, 6(10), 146. https://doi.org/10.3390/infrastructures6100146

[2] Agatonovic-Kustrin, S., & Beresford, R. (2000). Basic concepts of artificial neural network (ANN) modeling and its application in pharmaceutical research. Journal of Pharmaceutical and Biomedical Analysis, 22(5), 717–727. https://doi.org/10.1016/s0731-7085(99)00272-1

[3] Ahmad, A., Ahmad, W., Aslam, F., & Joyklad, P. (2022). Compressive strength prediction of fly ash-based geopolymer concrete via advanced machine learning techniques. Case Studies in Construction Materials, 16. https://doi.org/10.1016/j.cscm.2021.e00840

[4] Ahmad, A., Ahmad, W., Chaiyasarn, K., Ostrowski, K., Aslam, F., Zajdel, P., & Joyklad, P. (2021). Prediction of Geopolymer Concrete Compressive Strength Using Novel Machine Learning Algorithms. Polymers.

[5] Ahmed, A., Kumar, S. S., & Nanda, R. P. (2021). Development of geopolymer concrete mixes with ambient air curing. IOP Conference Series: Materials Science and Engineering, 1116(1), 12160. https://doi.org/10.1088/1757-899x/1116/1/012160

[6] Albitar, M., Mohamed Ali, M. S., Visintin, P., & Drechsler, M. (2017). Durability evaluation of geopolymer and conventional concretes. Construction and Building Materials. https://doi.org/10.1016/j.conbuildmat.2017.01.056

[7] Amin, M., Khan, K., Javed, M., Aslam, F., Qadir, M. G., & Faraz, M. I. (2022). Prediction of Mechanical Properties of Fly-Ash/Slag-Based Geopolymer Concrete Using Ensemble and Non-Ensemble Machine-Learning Techniques. Materials.

[8] Anuradha, R., Sreevidya, V., & Venkatasubramani, R. (2013). Microstructure of Geopolymer Concrete Based on Fly Ash Using M-Sand. Asian Journal of Chemistry, 25(2), 1095–1097. https://doi.org/10.14233/ajchem.2013.13522

[9] Asayesh, S., Shirzadi Javid, A. A., Ziari, H., & Mehri, B. (2021). Evaluating fresh state, hardened State, thermal expansion and bond properties of geopolymers for the repairing of concrete pavements under restrained conditions. Construction and Building Materials, 292, 123398. https://doi.org/10.1016/j.conbuildmat.2021.123398

[10] Awoyera, P. O., Kirgiz, M. S., Viloria, A., & Ovallos-Gazabon, D. (2020). Estimating strength properties of geopolymer self-compacting concrete using machine learning techniques. Journal of Materials Research and Technology, 9(4). https://doi.org/10.1016/j.jmrt.2020.06.008

[11] Banerjee, S., Gelfand, A. E., Finley, A. O., & Sang, H. (2008). Gaussian Predictive Process Models for Large Spatial Data Sets. Journal of the Royal Statistical Society Series B: Statistical Methodology, 70(4), 825–848. https://doi.org/10.1111/j.1467-9868.2008.00663.x

[12] Ben Chaabene, W., Flah, M., & Nehdi, M. L. (2020). Machine learning prediction of mechanical properties of concrete: Critical review. Construction and Building Materials. https://doi.org/10.1016/j.conbuildmat.2020.119889

[13] Chen, Y.-C., Lee, W.-H., & Ding, Y.-C. (2021). The Use of Recycled Aggregate Sludge for the Preparation of GGBFS and Fly Ash Based Geopolymer. Crystals, 11(12), 1486. https://doi.org/10.3390/cryst11121486

[14] Cheng, M.-Y., Huang, C.-C., & Roy, A. F. Van. (2014). PREDICTING PROJECT SUCCESS IN CONSTRUCTION USING AN EVOLUTIONARY GAUSSIAN PROCESS INFERENCE MODEL. Journal of Civil Engineering and Management, 19(Supplement_1), S202–S211. https://doi.org/10.3846/13923730.2013.801919

[15] da Paixão, R. C. F., Penido, R. E. K., Cury, A. A., & Mendes, J. C. (2022). Comparison of machine learning techniques to predict the compressive strength of concrete and considerations on model generalization. Revista IBRACON de Estruturas e Materiais, 15(5). https://doi.org/10.1590/S1983-41952022000500003

[16] Davidovits, J. (1994). Properties of Geopolymer Cements. First International Conference on Alkaline Cements and Concretes.

[17] de Brito, J., & Kurda, R. (2021). The past and future of sustainable concrete: A critical review and new strategies on cement-based materials. Journal of Cleaner Production, 281, 123558. https://doi.org/10.1016/j.jclepro.2020.123558

[18] Deb, P. S., Nath, P., & Sarker, P. K. (2014). The effects of ground granulated blast-furnace slag blending with fly ash and activator content on the workability and strength properties of geopolymer concrete cured at ambient temperature. Materials & Design (1980-2015), 62, 32–39. https://doi.org/10.1016/j.matdes.2014.05.001

[19] Ding, Y., Shi, C.-J., & Li, N. (2018). Fracture properties of slag/fly ash-based geopolymer concrete cured in ambient temperature. Construction and Building Materials, 190, 787–795. https://doi.org/10.1016/j.conbuildmat.2018.09.138

[20] Duxson, P., Fernández-Jiménez, A., Provis, J. L., Lukey, G. C., Palomo, A., & van Deventer, J. S. J. (2006). Geopolymer technology: the current state of the art. Journal of Materials Science, 42(9), 2917–2933. https://doi.org/10.1007/s10853-006-0637-z

[21] Esparham, A., & Mohammadi, M. (2022). Effect of Alkaline Solutions on Bentonite-Based Eco-Friendly Geopolymer Composite. ALKHAS The Journal of Environment Agriculture and Biological Sciences. https://doi.org/10.47176/alkhass.4.1.5

[22] Fang, G., Ho, W. K., Tu, W., & Zhang, M. (2018). Workability and mechanical properties of alkali-activated fly ash-slag concrete cured at ambient temperature. Construction and Building Materials, 172, 476–487. https://doi.org/10.1016/j.conbuildmat.2018.04.008

[23] Faridmehr, I., Nehdi, M. L., Huseien, G. F., Baghban, M. H., Sam, A. R. M., & Algaifi, H. A. (2021). Experimental and Informational Modeling Study of Sustainable Self-Compacting Geopolymer Concrete. Sustainability, 13(13), 7444. https://doi.org/10.3390/su13137444

[24] Ferdous, W., Manalo, A., Khennane, A., & Kayali, O. (2015). Geopolymer concrete-filled pultruded composite beams - Concrete mix design and application. Cement and Concrete Composites. https://doi.org/10.1016/j.cemconcomp.2014.12.012

[25] Garces, J. I. T., Dollente, I. J., Beltran, A. B., Tan, R. R., & Promentilla, M. A. B. (2021). Life cycle assessment of self-healing geopolymer concrete. Cleaner Engineering and Technology, 4, 100147. https://doi.org/10.1016/j.clet.2021.100147

[26] Gunasekara, C., Sandanayake, M., Zhou, Z., Law, D. W., & Setunge, S. (2020). Effect of nano-silica addition into high volume fly ash–hydrated lime blended concrete. Construction and Building Materials, 253, 119205. https://doi.org/10.1016/j.conbuildmat.2020.119205

[27] Gupta, A., Gupta, N., & Saxena, K. K. (2021). Mechanical and Durability Characteristics Assessment of Geopolymer Composite (GPC) at Varying Silica Fume Content. Journal of Composites Science, 5(9), 237. https://doi.org/10.3390/jcs5090237

[28] Hadi, M. N. S., Farhan, N. A., & Sheikh, M. N. (2017). Design of geopolymer concrete with GGBFS at ambient curing condition using Taguchi method. Construction and Building Materials, 140, 424–431. https://doi.org/10.1016/j.conbuildmat.2017.02.131

[29] Haruna H.; Umar, I.; Shao, J.; Adamu, M.; Ibrahim, Y., S. I. . Z. (2022). Gaussian process regression model for the prediction of the compressive strength of polyurethane-based polymer concrete for runway repair: A comparative approach. IOP Conference Series: Earth and Environmental Science, 1026. https://doi.org/10.1088/1755-1315/1026/1/012007

[30] John, S. K., Cascardi, A., Nadir, Y., Aiello, M. A., & Girija, K. (2021). A New Artificial Neural Network Model for the Prediction of the Effect of Molar Ratios on Compressive Strength of Fly Ash-Slag Geopolymer Mortar. Advances in Civil Engineering, 2021(1). https://doi.org/10.1155/2021/6662347

[31] Kanagaraj, B., N, A., Alengaram, U. J., Raj R, S., B, P., & Tattukolla, K. (2022). Performance evaluation on engineering properties and sustainability analysis of high strength geopolymer concrete. Journal of Building Engineering, 60, 105147. https://doi.org/10.1016/j.jobe.2022.105147

[32] Khokhar, S. A., Ahmed, T., Khushnood, R. A., Ali, S. M., & Shahnawaz. (2021). A Predictive Mimicker of Fracture Behavior in Fiber Reinforced Concrete Using Machine Learning. Materials, 14(24), 7669. https://doi.org/10.3390/ma14247669

[33] Kishore, Y. S. N., Nadimpalli, S. G. D., Potnuru, A. K., Vemuri, J., & Khan, M. A. (2022). Statistical analysis of sustainable geopolymer concrete. Materials Today: Proceedings, 61, 212–223. https://doi.org/10.1016/j.matpr.2021.08.129

[34] Kumar, A., Arora, H. C., Kapoor, N. R., Mohammed, M. A., Kumar, K., Majumdar, A., & Thinnukool, O. (2022). Compressive Strength Prediction of Lightweight Concrete: Machine Learning Models. Sustainability (Switzerland), 14(4). https://doi.org/10.3390/su14042404

[35] Kumar, B. S. C. (2019). Correlation between Compressive Strength and Split Tensile Strength of GGBS and MK Based Geopolymer Concrete using Regression Analysis. JOURNAL OF MECHANICS OF CONTINUA AND MATHEMATICAL SCIENCES, 14(1). https://doi.org/10.26782/jmcms.2019.02.00002

[36] Kurhade S., S. . P. (2024). Predicting compressive strength of geopolymer concrete using machine learning models. Innovative Infrastructure Solutions. https://doi.org/10.1007/s41062-024-01832-8

[37] Lee, W.-H., Lin, K.-L., Chang, T.-H., Ding, Y.-C., & Cheng, T.-W. (2020). Sustainable Development and Performance Evaluation of Marble-Waste-Based Geopolymer Concrete. Polymers, 12(9), 1924. https://doi.org/10.3390/polym12091924

[38] Liu, J., Shi, X., Zhang, G., & Li, L. (2023). Study the Mechanical Properties of Geopolymer under Different Curing Conditions. Minerals.

[39] Lopes, A. V, Lopes, S. M. R., & Pinto, I. (2020). Influence of the Composition of the Activator on Mechanical Characteristics of a Geopolymer. Applied Sciences, 10(10), 3349. https://doi.org/10.3390/app10103349

[40] Ma, C.-K., Awang, A. Z., & Omar, W. (2018). Structural and material performance of geopolymer concrete: A review. Construction and Building Materials, 186, 90–102. https://doi.org/10.1016/j.conbuildmat.2018.07.111

[41] Malayali, A. B., Chokkalingam, R. B., & Muthukannan, M. (2021). Strength Properties of Geopolymer Concrete Modified with Recycled Aggregates. Iranian Journal of Science and Technology, Transactions of Civil Engineering, 46(1), 77–89. https://doi.org/10.1007/s40996-021-00662-3

[42] Mineral Commodity Summaries 2019. (2019). In Mineral Commodity Summaries. US Geological Survey. https://doi.org/10.3133/70202434

[43] Mohammed Hameed, M., & Mohammed Ali, A. (2021). Using of metakaolin to produce colored geopolymer concrete. Journal of Physics: Conference Series, 2114(1), 12018. https://doi.org/10.1088/1742-6596/2114/1/012018

[44] Montes, C., & Allouche, E. N. (2013). Rheological Behavior of Fly-Ash-Based Geopolymers. In Geopolymer Binder Systems (pp. 72–84). ASTM International. https://doi.org/10.1520/stp156620120094

[45] Mustafa, M. A.-T., Hanafi, I., Mahmoud, R., & Tayeh, B. A. (2019). Effect of partial replacement of sand by plastic waste on impact resistance of concrete: experiment and simulation. Structures, 20, 519–526. https://doi.org/10.1016/j.istruc.2019.06.008

[46] N.d., H. G. G. (2022). Cement Industry Initiative Releases Technology Roadmap to Cut CO2 Emissions 24% by 2050. SDG Knowledge Hub | IISD.

[47] Naghizadeh, A., & Ekolu, S. O. (2019). Method for comprehensive mix design of fly ash geopolymer mortars. Construction and Building Materials. https://doi.org/10.1016/j.conbuildmat.2018.12.185

[48] Nath, P., & Sarker, P. K. (2015). Use of OPC to improve setting and early strength properties of low calcium fly ash geopolymer concrete cured at room temperature. Cement and Concrete Composites, 55, 205–214. https://doi.org/10.1016/j.cemconcomp.2014.08.008

[49] Nath, P., & Sarker, P. K. (2017). Flexural strength and elastic modulus of ambient-cured blended low-calcium fly ash geopolymer concrete. Construction and Building Materials, 130, 22–31. https://doi.org/10.1016/j.conbuildmat.2016.11.034

[50] Noble, W. S. (2006). What is a support vector machine? Nature Biotechnology, 24(12), 1565–1567. https://doi.org/10.1038/nbt1206-1565

[51] Omran, B. A., Chen, Q., & Jin, R. (2016). Comparison of Data Mining Techniques for Predicting Compressive Strength of Environmentally Friendly Concrete. Journal of Computing in Civil Engineering, 30(6). https://doi.org/10.1061/(asce)cp.1943-5487.0000596

[52] Oti, J., Adeleke, B., Anowie, F. X., Kinuthia, J. M., & Ekwulo, E. (2024). Mechanical Properties of a Sustainable Low-Carbon Geopolymer Concrete Using a Pumice-Derived Sodium Silicate Solution. Materials.

[53] Padakanti, R., Sarella, V. R., Pancharathi, R. K., & Jha, A. (2022). Study on the bond behavior of high-strength geopolymer concrete. Asian Journal of Civil Engineering, 23(2), 269–288. https://doi.org/10.1007/s42107-022-00422-2

[54] Pan, Z., Sanjayan, J. G., & Rangan, B. V. (2011). Fracture properties of geopolymer paste and concrete. Magazine of Concrete Research, 63(10), 763–771. https://doi.org/10.1680/macr.2011.63.10.763

[55] Panda, B., & Tan, M. J. (2018). Experimental study on mix proportion and fresh properties of fly ash based geopolymer for 3D concrete printing. Ceramics International. https://doi.org/10.1016/j.ceramint.2018.03.031

[56] Patel, Y. J., & Shah, N. (2018). Development of self-compacting geopolymer concrete as a sustainable construction material. Sustainable Environment Research, 28(6), 412–421. https://doi.org/10.1016/j.serj.2018.08.004

[57] Pham, T. M., Liu, J., Tran, P., Pang, V.-L., Shi, F., Chen, W., Hao, H., & Tran, T. M. (2020). Dynamic compressive properties of lightweight rubberized geopolymer concrete. Construction and Building Materials, 265, 120753. https://doi.org/10.1016/j.conbuildmat.2020.120753

[58] Philip, S., Nidhi, M., & Ahmed, H. U. (2024). A comparative analysis of tree-based machine learning algorithms for predicting the mechanical properties of fibre-reinforced GGBS geopolymer concrete. Multiscale and Multidisciplinary Modeling, Experiments and Design, 7(3). https://doi.org/10.1007/s41939-023-00355-6

[59] Put, R., Perrin, C., Questier, F., Coomans, D., Massart, D. L., & Vander Heyden, Y. (2003). Classification and regression tree analysis for molecular descriptor selection and retention prediction in chromatographic quantitative structure–retention relationship studies. Journal of Chromatography A, 988(2), 261–276. https://doi.org/10.1016/s0021-9673(03)00004-9

[60] Rahman, S. K., & Al-Ameri, R. (2021). A newly developed self-compacting geopolymer concrete under ambient condition. Construction and Building Materials, 267, 121822. https://doi.org/10.1016/j.conbuildmat.2020.121822

[61] Rahmawati, C., Aprilia, S., Saidi, T., Aulia, T. B., & Hadi, A. E. (2021). The Effects of Nanosilica on Mechanical Properties and Fracture Toughness of Geopolymer Cement. Polymers, 13(13), 2178. https://doi.org/10.3390/polym13132178

[62] Rashiddadash, P., Ramezanianpour, A. A., & Mahdikhani, M. (2014). Experimental investigation on flexural toughness of hybrid fiber reinforced concrete (HFRC) containing metakaolin and pumice. Construction and Building Materials, 51, 313–320. https://doi.org/10.1016/j.conbuildmat.2013.10.087

[63] Reddy, M. S., Dinakar, P., & Rao, B. H. (2018). Mix design development of fly ash and ground granulated blast furnace slag based geopolymer concrete. Journal of Building Engineering, 20, 712–722. https://doi.org/10.1016/j.jobe.2018.09.010

[64] Rehman, A., & Khokhar, I. (2022). ANN based predictive mimicker for mechanical and rheological properties of eco-friendly geopolymer concrete. Case Studies in Construction Materials.

[65] Ren, Q., Ding, L., Dai, X., Jiang, Z., & De Schutter, G. (2021). Prediction of Compressive Strength of Concrete with Manufactured Sand by Ensemble Classification and Regression Tree Method. Journal of Materials in Civil Engineering, 33(7). https://doi.org/10.1061/(asce)mt.1943-5533.0003741

[66] Simatupang, P. H., Nine, V., & Sinaga, A. E. (2019). Setting time and compression strength of low-calcium fly ash geopolymer paste with non-calcined red soil substitution in ambient curing. IOP Conference Series: Materials Science and Engineering, 669(1), 12025. https://doi.org/10.1088/1757-899x/669/1/012025

[67] Sitarz, M., Castro-Gomes, J., & Hager, I. (2021). Strength and Microstructure Characteristics of Blended Fly Ash and Ground Granulated Blast Furnace Slag Geopolymer Mortars with Na and K Silicate Solution. Materials, 15(1), 211. https://doi.org/10.3390/ma15010211

[68] Sitarz, M., Hager, I., & Choińska, M. (2020). Evolution of Mechanical Properties with Time of Fly-Ash-Based Geopolymer Mortars under the Effect of Granulated Ground Blast Furnace Slag Addition. Energies, 13(5), 1135. https://doi.org/10.3390/en13051135

[69] Sivasundaram, V., & Malhotra, V. M. (1988). Fly ash in concrete compilation of abstracts of papers from recent international conferences and symposia on fly ash in concrete. Natural Resources Canada/CMSS/Information Management. https://doi.org/10.4095/305072

[70] Somna, K., Jaturapitakkul, C., Kajitvichyanukul, P., & Chindaprasirt, P. (2011). NaOH-activated ground fly ash geopolymer cured at ambient temperature. Fuel. https://doi.org/10.1016/j.fuel.2011.01.018

[71] Sravanthi, D., Himath Kumar, Y., & Sarath Chandra Kumar, B. (2020). Comparative study on flow characteristics, strength and durability of GGBS based geopolymer concrete. IOP Conference Series: Materials Science and Engineering, 912(6), 62032. https://doi.org/10.1088/1757-899x/912/6/062032

[72] Subash, N., Avudaiappan, S., Adish Kumar, S., Amran, M., Vatin, N., Fediuk, R., & Aepuru, R. (2021). Experimental Investigation on Geopolymer Concrete with Various Sustainable Mineral Ashes. Materials, 14(24), 7596. https://doi.org/10.3390/ma14247596

[73] Topçu, İ. B., & Sarıdemir, M. (2008). Prediction of compressive strength of concrete containing fly ash using artificial neural networks and fuzzy logic. Computational Materials Science, 41(3), 305–311. https://doi.org/10.1016/j.commatsci.2007.04.009

[74] Van Dao, D., Ly, H. B., Trinh, S. H., Le, T. T., & Pham, B. T. (2019). Artificial intelligence approaches for prediction of compressive strength of geopolymer concrete. Materials. https://doi.org/10.3390/ma12060983

[75] Venkatesh, C., Rao, M. V. S., Praveen Kumar, M., & Sonali Sri Durga, C. (2024). Effect of mineral admixtures and curing regimes on propertieof self-compacting concrete. Journal of Sustainable Construction Materials and Technologies, 9(1). https://doi.org/10.47481/jscmt.1383493

[76] Verma, M., Upreti, K., Vats, P., Singh, S., Singh, P., Dev, N., Kumar Mishra, D., & Tiwari, B. (2022). Experimental Analysis of Geopolymer Concrete: A Sustainable and Economic Concrete Using the Cost Estimation Model. Advances in Materials Science and Engineering, 2022, 1–16. https://doi.org/10.1155/2022/7488254

[77] Wang, Q., Bian, H., Li, M., Dai, M., Chen, Y., Jiang, H., Zhang, Q., Dong, F., Huang, J., & Ding, Z. (2022). Effects of a Water-Glass Module on Compressive Strength, Size Effect and Stress–Strain Behavior of Geopolymer Recycled Aggregate Concrete. Crystals, 12(2), 218. https://doi.org/10.3390/cryst12020218

[78] Wang, W.-C., Wang, H.-Y., & Lo, M.-H. (2015). The fresh and engineering properties of alkali activated slag as a function of fly ash replacement and alkali concentration. Construction and Building Materials, 84, 224–229. https://doi.org/10.1016/j.conbuildmat.2014.09.059

[79] Waqas, R. M., Butt, F., Danish, A., Alqurashi, M., Mosaberpanah, M. A., Masood, B., & Hussein, E. E. (2021). Influence of Bentonite on Mechanical and Durability Properties of High-Calcium Fly Ash Geopolymer Concrete with Natural and Recycled Aggregates. Materials, 14(24), 7790. https://doi.org/10.3390/ma14247790

[80] Waqas, R. M., Butt, F., Zhu, X., Jiang, T., & Tufail, R. F. (2021). A Comprehensive Study on the Factors Affecting the Workability and Mechanical Properties of Ambient Cured Fly Ash and Slag Based Geopolymer Concrete. Applied Sciences, 11(18), 8722. https://doi.org/10.3390/app11188722

[81] Yilmaz, Y., Cakmak, T., Kurt, Z., & Ustabas, I. (2024). Predicting Mechanical Properties in Geopolymer Mortars, Including Novel Precursor Combinations, Through XGBoost Method. Arabian Journal for Science and Engineering.

[82] Zaidahtulakmal, M. Z., Kartini, K., & Hamidah, M. S. (2019). Rice husk ash (RHA) based geopolymer mortar incorporating sewage sludge ash (SSA). Journal of Physics: Conference Series, 1349(1), 12022. https://doi.org/10.1088/1742-6596/1349/1/012022

[83] Zhang, H., Li, L., Yuan, C., Wang, Q., Sarker, P. K., & Shi, X. (2020). Deterioration of ambient-cured and heat-cured fly ash geopolymer concrete by high temperature exposure and prediction of its residual compressive strength. Construction and Building Materials, 262, 120924. https://doi.org/10.1016/j.conbuildmat.2020.120924

[84] Zhang, P., Sun, X., Wang, F., & Wang, J. (2023). Mechanical Properties and Durability of Geopolymer Recycled Aggregate Concrete: A Review. Polymers.

[85] Zhao, J., Wang, K., Wang, S., Wang, Z., Yang, Z., Shumuye, E. D., & Gong, X. (2021). Effect of Elevated Temperature on Mechanical Properties of High-Volume Fly Ash-Based Geopolymer Concrete, Mortar and Paste Cured at Room Temperature. Polymers, 13(9), 1473. https://doi.org/10.3390/polym13091473